

## Characterization of FUSI-PtSi Formed on Ultrathin HfO<sub>2</sub>/Si(100) by Photoelectron Spectroscopy

Y. Munetaka<sup>1</sup>, F. Takeno<sup>1</sup>, A. Ohta<sup>1</sup>, H. Murakami<sup>1</sup>, S. Higashi<sup>1</sup>,  
S. Miyazaki<sup>1</sup>, M. Kadoshima<sup>2</sup> and T. Nabatame<sup>2</sup>

<sup>1</sup>Graduate School of Advanced Sciences of Matter, Hiroshima University,

Kagamiyama 1-3-1, Higashi-Hiroshima

Fax: +81-082-422-7038, e-mail: semicon@hiroshima-u.ac.jp

<sup>2</sup>MIRAI-ASET Onogawa16-1, Tsukuba

We studied the work function of fully silicided (FUSI) PtSi formed on ultrathin HfO<sub>2</sub> as a function of chemical composition by using X-ray photoelectron spectroscopy (XPS). In evaluating the work function, the threshold energy for photoelectrons near the lower limit in the kinetic energy scale was determined by fitting a Fowler function to the measured spectra, and cross-checked by total photoelectron yield measurements. In sample preparation, after chemical vapor deposition of 100nm-thick undoped amorphous-Si on 2nm-thick HfO<sub>2</sub>/n-Si(100), a 100nm-thick Pt layer was formed on the a-Si layer by sputtering and followed by silicidation at 400°C. In the Pt-rich near-surface region in which the Pt content is in the range of 65-73 at.%, the work function was determined to be 5.0eV within an accuracy of 100meV. With progressive low energy Ar<sup>+</sup> ion sputtering, the work function is gradually decreased and constant at ~4.8eV in the region with stoichiometric composition (50%). Notice that in the region near the interface, a photoemission component with a threshold energy as low as ~4.65eV becomes observable in a manner that overlaps with the photoemission from PtSi, which is attributable to the photoemission from the conduction band of the n-Si (100) substrate.

Key words: XPS, full silicided gate, platinum silicide, work function

### 1. INTRODUCTION

Continuous scaling of complementary metal-oxide-semiconductor field effect transistors (CMOSFETs) inevitably requires an increase in capacitive coupling between the gate and the channel while maintaining an allowable leakage current level through a gate dielectric. In this regard, many efforts have been made to replace conventional silicon oxynitride with physically thicker but electrically thinner high-k gate dielectrics [1-3]. Meanwhile, the use of conventional poly-Si gate is faced practically with serious limitations related to gate potential drop caused by the gate leakage current flowing through a gate resistance [4], a depletion effect [5,6] and a Fermi level pinning [7,8] phenomenon emerging in combination with high-k gate dielectrics. To overcome such limitations, the implementation of alternative gate materials with lower resistivity is needed. Silicides such as NiSi are thought to be promising candidates for metal gates [9-11]. The control of the work function of silicides is one of the major issues for the use of silicide/high-k dielectric gate stacks. Although the work function of silicides can be controlled to some extent by a change in chemical composition and/or impurity doping, even in the case of NiSi in which the Fermi level is located inherently around the Si midgap, it is difficult to obtain the values suitable for n- and p-MOSFETs [11].

For pMOSFETs, Pt mono-silicide (PtSi) is thought to be an alternative gate material because of its work function as high as 4.9eV[12].

In this work, we focused on depth profiling of chemical composition and the work function for PtSi formed on HfO<sub>2</sub> by full silicidation of a-Si by combination of X-ray photoelectron spectroscopy (XPS) and low energy Ar<sup>+</sup> ion etching.

### 2. EXPERIMENTAL

After standard wet-cleaning steps of the n-type Si(100) wafers, a 1.0nm-thick SiO<sub>2</sub> interfacial layer was grown on the surface by thermal oxidation at 900°C. 2.0nm-thick HfO<sub>2</sub> film was formed by an atomic layer deposition (ALD) technique at a temperature of 250°C, where tetrakis-di-methyl-amino-hafnium (Hf[N(CH<sub>3</sub>)<sub>2</sub>]<sub>4</sub>) and H<sub>2</sub>O were used as precursors. To densify the HfO<sub>2</sub> films, the post-deposition anneal was carried out at 850°C in O<sub>2</sub> ambience. Subsequently, a 100nm-thick undoped amorphous-Si was deposited by LPCVD and followed by deposition of a 100nm-thick Pt film was deposited by sputtering on a-Si layer. Finally, the stack structure was silicided at 400°C in Ar atmosphere, with the result that a 190nm-thick fully-silicided PtSi was formed.

Raman scattering spectroscopy, in which a

p-polarized laser light with a wavelength of 531.2nm is incident at a glancing angle of  $\sim 10^\circ$ , was performed to evaluate the chemical structure of the so-prepared PtSi layer. For the depth profiling of the chemical and electronic structures of PtSi, XPS measurements using monochromatized AlK $\alpha$  radiation ( $h\nu=1486.71\text{eV}$ ) were performed at each step of PtSi thinning by a low energy Ar<sup>+</sup> beam. In evaluating the work function of PtSi, the threshold energy for photoelectrons near the lower limit in the kinetic energy scale, in other words the upper limit in the binding energy scale, was determined by fitting Fowler function to the measured spectra, and also cross-checked by total photoelectron yield spectroscopy (PYS) [13].

### 3. RESULTS AND DISCUSSION

#### 3.1 Characterization of chemical structure for FUSI-PtSi

Figure 1 shows a Raman spectrum for FUSI-PtSi just after silicidation. Obviously, PtSi signals were mainly observed around  $140\text{cm}^{-1}$  in Raman shift and Pt<sub>2</sub>Si signals were slightly observable around  $90\text{cm}^{-1}$  [14], which implies that Pt-rich PtSi was formed at the surface as also confirmed by XPS measurements. The changes in the Pt4f and Si2p spectra for PtSi with progressive thinning by Ar<sup>+</sup> ion sputtering are shown in Fig. 2. In the early stages of Ar<sup>+</sup> ion sputtering, a Pt-rich component peaked at  $\sim 71.6\text{eV}$  was mainly observed. Through Ar<sup>+</sup> ion sputtering for 5min, no C1s signal was able to be detected. With progressive Ar<sup>+</sup> ion sputtering, the Pt-rich component is decreased monotonously, while the Pt4f signals at  $\sim 74\text{eV}$  due to Pt-Si bonding units become significant until 90 min in sputtering time and then gradually decreased. In the Si2p spectra within 60 min in sputtering time, one can see a distinct Pt-Si component accompanied by weak signals due to oxidized Si bonds in the higher binding energy side. Through Ar<sup>+</sup> sputtering for 90 min, signals peaked at  $\sim 99.4\text{eV}$  originating from the Si(100) substrates

become observable, and the intensity of the substrate component increases with further progressive sputtering. Taking into account photo-ionized cross-sections of Si2p and Pt 4f photoelectrons and the kinetic energy dependence of photoelectron escape depth, the depth profile of the chemical composition in the PtSi layer was roughly estimated from the change in the core-line spectra with progressive Ar<sup>+</sup> ion sputtering as shown in Fig. 3. As a result, PtSi is formed under a Pt-rich surface region.

#### 3.2 Evaluation of the work function for PtSi

We first checked the work function of the PtSi surface by PYS measurements (Fig. 4). The measured PYS spectrum was likely to consist of some components with different photoelectric threshold energies. To determine the lowest threshold, we took two approaches. The first was by linear extrapolation in square root of the photoelectron yield as a function of photon energy as shown in Fig. 4 (a), through which the surface work function was determined to be 5.05eV. The other was by fitting a Fowler function to the measured yield spectrum as shown in Fig. 4 (b), through which a work function value of  $5.0\pm 0.05\text{eV}$

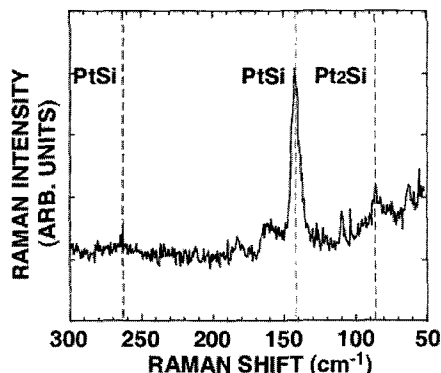


Fig. 1. Raman scattering spectrum for FUSI-PtSi(190nm) formed on HfO<sub>2</sub>(2nm)/SiO<sub>2</sub>(1nm)/Si(100) measured under a right-angle scattering geometry.

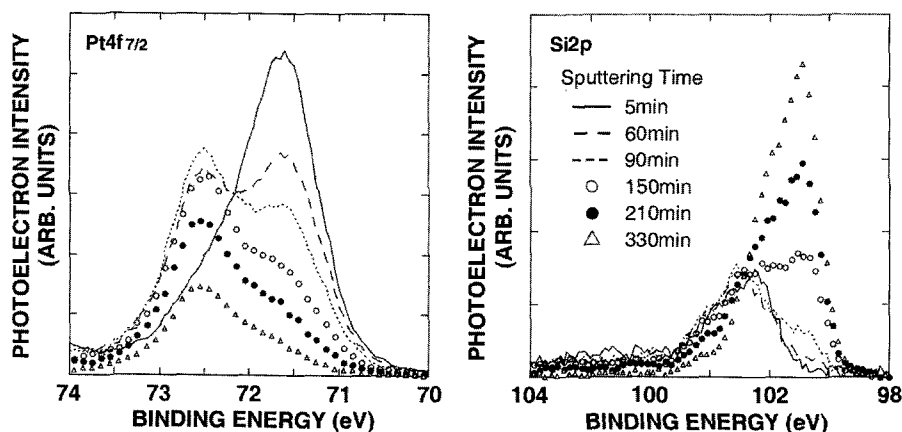


Fig. 2. Pt4f 7/2 and Si2p taken at each thinning step of the FUSI-PtSi layer with Ar<sup>+</sup> ion sputtering. The photoelectron take-off angle was set at  $90^\circ$ .

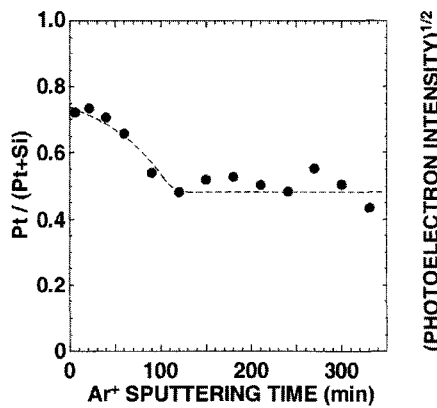


Fig. 3. Depth profiles of Pt/(Pt+Si) ratio in the FUSI-PtSi layer.

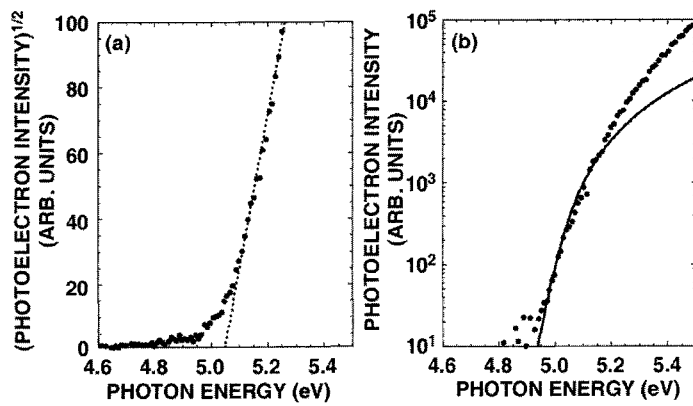


Fig. 4. A total photoelectron yield spectrum for the FUSI-PtSi layer. The square root plot of the spectrum (a) and the semi-logarithmic plot (b) are represented. The well-fitted Fowler function (solid line) is also shown in (b).

was obtained from the energy shift for a good fitting to the measured yield near the threshold energy. Thus, we can conclude the work function of the Pt-rich surface to be 5.0-5.1eV, being rather close to the reported value for Pt-monosilicide.

To conduct depth profiling of the work function in the Pt-silicide layer in parallel with chemical composition analysis by XPS measurements at each step of Ar<sup>+</sup> ion sputtering, the lower limit in the kinetic energy scale, or the upper limit in the binding energy scale, was carefully monitored during XPS measurements. Photo-excited electrons passing through materials can suffer inelastic scatterings and lose their energy with some electronic excitations. If the kinetic energy of excited electrons becomes or is below the work function of a metallic material of interest, such a low energy electron can no longer emit to the outside. Thus, the work function can be determined from the threshold energy for photoelectrons near the lower limit in the kinetic energy scale. With consideration of the Fermi distribution at room temperature, based on the Fowler theory, we determined the work function from the energy shift by which was fitted a Fowler function at room temperature to the measured photoelectron spectrum near the lower limit in the kinetic energy scale [15]. In this work, to detect sufficient photoelectrons emitting with a low kinetic energy, negative bias as low as -15V was applied to the sample. For the calibration of this technique and setting a proper sample bias, we first measured the work functions of pure metals such as Au, Ni and Pt and confirmed that the measured values are the same as the reported ones within an accuracy of  $\pm 0.05\text{eV}$  just after evaporation or after removing surface carbon contaminants by Ar<sup>+</sup> ion sputtering.

Figure 5 shows the change in the spectrum near the lower limit in the kinetic energy scale for FUSI-PtSi with progressive Ar<sup>+</sup> sputtering. The Fermi edge is gradually shifted toward the lower kinetic energy side with increasing Ar<sup>+</sup> ion sputtering time. By

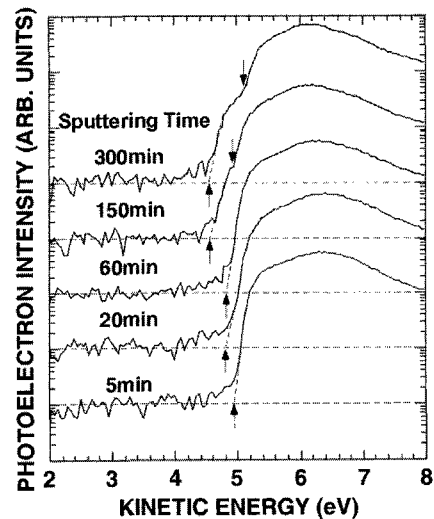


Fig. 5. The spectra near the Fermi edge for the FUSI-PtSi layer taken at different times in Ar<sup>+</sup> ion sputtering.

sputtering for 150 min and longer, the subsidiary onset becomes observable in the higher kinetic energy side. As represented in Fig. 6, by fitting a Fowler function to the measured spectra, a single threshold was determined to be 5.01eV, obtained after 5 min of sputtering, and the two thresholds (4.86 and 4.65eV) were obtained after 300 min of sputtering. Figure 7 shows depth profiling of threshold energies in the FUSI-PtSi stacked structure. In the Pt-rich near surface region, the work function was determined to  $5.0 \pm 0.05\text{eV}$ . With progressive Ar<sup>+</sup> ion sputtering, the work function gradually decreased and was constant at 4.85eV. Notice that in the region near the interface where Si2p signals from the Si (100) substrate are observable, a photoemission component with a threshold energy as low as  $\sim 4.65\text{eV}$  becomes observable in a manner that overlaps with the photoemission from PtSi, which can be interpreted in

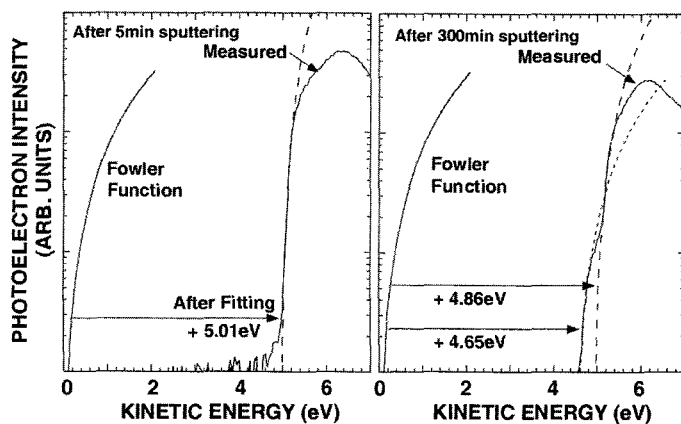


Fig. 6. Curve fittings to the measured spectra near the Fermi edge with the use of a Fowler function for the cases after  $\text{Ar}^+$  sputtering for 5 and 300 min.

terms of the electron emission from the Si conduction band as displayed in the inset.

#### 4. CONCLUSIONS

We have evaluated the depth profile of chemical composition and work function for FUSI-PtSi/ $\text{HfO}_2$  stacked structures. In the Pt-rich near surface region with a Pt content in the range of 65~73%,  $\text{Pt}_2\text{Si}$  phase and Pt-Pt bonds were detected, and a Pt mono-silicide phase was formed near the PtSi/ $\text{HfO}_2$  interface as shown by Raman spectrum and XPS measurements, respectively. The work function of the Pt-rich surface was determined to be ~5.0eV. With progressive  $\text{Ar}^+$  ion sputtering, the work function gradually decreased and was constant at ~4.85eV in the PtSi stoichiometric region. In the region near the interface, a photoemission component with a threshold energy as low as ~4.65eV became observable, which is attributable to photoemission from the conduction band of the n-Si(100) substrate.

#### ACKNOWLEDGEMENT

This work was partly supported by NEDO/MIRAI project.

#### REFERENCES

- [1] M. Fukuda, W. Mizubayashi, A. Kohno, S. Miyazaki and M. Hirose, *Jpn. J. Appl. Phys.* **37**, L1534 (1998).
- [2] G.D. Wilk, R.M. Wallace and J.M. Anthony, *J. Appl. Phys.* **89**, p.5243 (2001).
- [3] M.L. Green, E.P. Gusev, R. Degraeve and E.L. Garfunkel, *J. Appl. Phys.* **90**, 2057 (2001).
- [4] M. Koh, W. Mizubayashi, K. Iwamoto, H. Murakami, T. Ono, M. Tsuno, T. Mihara, K. Shibahara, S. Miyazaki and M. Hirose, *IEEE Trans. Elect. Dev.* **48**, 259 (2001).
- [5] R. Rios, N.D. Arora, and C.-L. Huang,

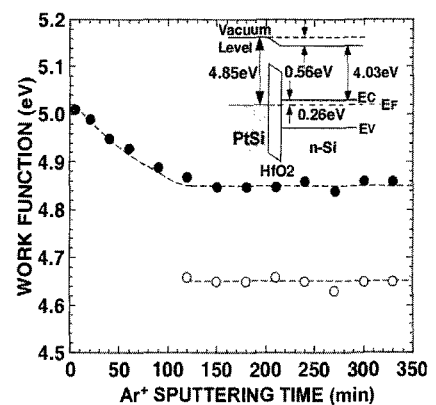


Fig. 7. Depth profiles of the photoelectron threshold energies determined by XPS measurements. The energy band diagram for the PtSi/ $\text{HfO}_2/\text{Si}(100)$  system is illustrated in the inset.

*IEEE Electron Device Lett.* **15**, 129 (1994).

- [6] N.D. Arora, R. Rios and C.-L. Huang, *IEEE Trans. Elect. Dev.* **42**, 935 (1995).
- [7] C. Hobbs, L. Fonseca, A. Knizhnik, V. Dhandapani, S. Samavadam, B. Taylor, J. Grant, L. Dip, D. Triyoso, R. Hegde, D. Gilmer, R. Garcia, D. Roan, L. Lovejoy, R. Rai, L. Hebert, H. Tseng, S. Anderson, B. White and P. Tobin, *IEEE Trans. Elect. Dev.* **51**, 978 (2004).
- [8] K. Shiraishi, K. Yamada, K. Torii, Y. Akasaka, K. Nakajima, M. Konno, T. Chikyow, H. Kitajima and T. Arikado, *Jpn. J. Appl. Phys.* **43**, L1413 (2004).
- [9] J. Kedzierski, E. Nowak, T. Kanarsky, Y. Zhang, D. Boyd, R. Carruthers, C. Cabral and R. Amos, *Tech. Dig. IEEE Int. Electron Device Meeting*, p.247 (San Francisco, 2002).
- [10] J. Kedzierski, D. Boyd, P. Ronsheim, S. Zafar, J. Newbury, J. Ott, C. Cabral Jr., M. Jeong and W. Haensch, *Tech. Dig. IEEE Int. Electron Devices Meeting*, p. 315 (Washington, 2003).
- [11] C. Cabral, Jr., J. Kedzierski, B. Linder, S. Zafer, V. Narayanan, S. Fang, A. Steegen, P. Kozlowski, R. Carruthers and R. Jammy, *VLSI Symp. Tech. Dig.* p.184 (2004).
- [12] M. Kadoshima, K. Akiyama, N. Mise, S. Migata, N. Yasuda, K. Iwamoto, H. Fujiwara, K. Tominaga, M. Ohno, T. Nabatame and A. Toriumi, *Ext. Abs. Int. Conf. on Solid State Device and Materials*, p. 466 (Tokyo, 2004).
- [13] S. Miyazaki, T. Maruyama, A. Kohno and M. Hirose, *Microelectron. Eng.* **48**, 63 (1999).
- [14] J.C. Tsang, Y. Yokota, R. Matz and G. Rubloff, *Appl. Phys. Lett.* **44**, p. 430 (1984).
- [15] F.U. Hillebrecht, J.C. Fuggle, P.A. Bennett and Z. Zolnierok, *Phys. Rev. B* **27**, 2179 (1983).

(Received December 29, 2005; Accepted January 31, 2006)